Polymer Degradation and Stability 159 (2019) 79–89

Contents lists available at ScienceDirect

Polymer Degradation and Stability

journal homepage: www.elsevier.com/locate/polydegstab

Synthesis of a DOPO-containing imidazole curing agent and its application in reactive flame retarded epoxy resin

Siqi Huo [a], Jun Wang [a, b], Shuang Yang [b, c, *], Chuan Li [d], Xiaolei Wang [d], Haopeng Cai [a, b]

[a] School of Materials Science and Engineering, Wuhan University of Technology, Wuhan, 430070, People's Republic of China
[b] Institute of Advanced Material Manufacturing Equipment and Technology, Wuhan University of Technology, Wuhan, 430070, People's Republic of China
[c] School of Mechanical and Electronic Engineering, Wuhan University of Technology, Wuhan, 430070, People's Republic of China
[d] Shanghai Composites Science & Technique Co., Ltd., Shanghai, 201112, People's Republic of China

ARTICLE INFO

Article history:
Received 9 September 2018
Received in revised form
10 November 2018
Accepted 18 November 2018
Available online 19 November 2018

Keywords:
Epoxy resin
Flame retardant
Phosphaphenanthrene
Imidazole

ABSTRACT

A novel DOPO-containing imidazole curing agent (DIB) was successfully synthesized, and served as a co-curing agent of 4,4'-diaminediphenyl sulfone (DDS) to prepare a reactive flame-retarded epoxy thermoset (EP/DDS/DIB). The DSC results showed that the curing temperature of EP/DDS/DIB mixture was much lower than that of EP/DDS mixture due to the catalytic curing effect of imidazole group. Although the T_g values of EP/DDS/DIB thermosets decreased in some degree, they were still obviously higher than that of EP/DDS/DOPO thermoset. The combustion tests indicated that DIB was a high-efficiency flame retardant for epoxy resin. The LOI value and UL94 rating of EP/DDS/DIB-0.75 sample reached 36.8% and V-0, respectively. In addition, the pk-HRR, av-HRR and THR of EP/DDS/DIB-1.0 thermoset were decreased by 57.2%, 37.9% and 36.0%, respectively, compared with those of EP/DDS thermoset. The studies concerning decomposition products in both condensed and gaseous phases revealed that the introduction of DIB brought about the formation of a protective intumescent char layer and the release of phosphorus-containing radicals and noncombustible nitrogen-containing fragments during combustion. DIB exerted bi-phase flame retardant effect on epoxy resin.

1. Introduction

Epoxy resin (EP), as one of advanced resin matrixes, had been widely applied in many fields such as coating, electronics, aerospace industry and so on [1–3]. Although EP possessed excellent adhesive properties, good mechanical behavior, great chemical resistance and superior insulation performance, its inflammability severely restricted its applications [4,5]. Therefore, flame-retardant EP had become a research hotspot in recent years.

Traditionally, the incorporation of halogen flame retardant was an effective way to improve the flame retardancy of EP [6]. Though the flame-retardant effect of halogen flame retardant was excellent, it generated a large amount of smoke, corrosive gases and toxic substances during combustion [7]. With increasing ecological and environmental concerns, the application of halogen flame-retardants was limited and halogen-free alternatives were developed rapidly [8–10].

For the past few years, phosphorus-containing flame retardant had become one of the most popular halogen-free flame retardants [11–14]. Among different kinds of phosphorus-containing flame retardants, 9,10-dihydro-9-oxa-10-phosphaphenanthrene-10-oxide (DOPO) and its derivatives were often used to improve the flame-retardant performance of EP [15–17]. As we all knew, DOPO-based flame retardants fell into two categories: additive and reactive types [18,19]. Compared with the additive flame retardants, the flame-retardant effect of reactive flame retardants could be maintained long-term since they were covalently linked with EP matrix [20]. However, the common DOPO-based flame retardants exhibited relatively lower flame retardant efficiency compared with synergistic flame retardant. Introducing other flame-retardant groups into DOPO-based flame retardants was an effective method to improve the flame-retardant efficiency [21–23]. In the past, the nitrogen heterocyclic rings such as triazine [24,25], triazole [26], thiazole [27,28] and maleimide [29,30], were integrated with DOPO group to prepare

---

* Corresponding author. Institute of Advanced material manufacturing equipment and technology, Wuhan University of Technology 122 Luoshi Road, Hongshan District, Wuhan, 430070, People's Republic of China.
E-mail address: ysfrp@whut.edu.cn (S. Yang).

https://doi.org/10.1016/j.polymdegradstab.2018.11.021

high-efficiency flame retardants, which was instructive for preparing DOPO-based synergistic flame retardants. In addition, the common DOPO-based reactive flame retardants have low curing activity with epoxy resin due to the steric hindrance effect, resulting in incomplete curing of EP thermoset [31,32].

Imidazole ring, as a heterocycle with high nitrogen content, was verified to have good thermal stability and be capable of curing epoxy resin efficiently [33,34]. Therefore, a high-efficiency flame retardant with good curing activity with epoxy resin might be prepared by integrating imidazole ring and DOPO group into one molecular structure.

Thus, in this work, a novel reactive flame retardant (DIB) with phosphaphenanthrene and imidazole groups was successfully synthesized from DOPO, 1H-imidazole-4-carbaldehyde, and 1,4-benzenediamine. DIB was used as a reactive flame retardant to prepare a reactive flame-retardant EP thermoset. The curing behaviors, thermal properties, flame retardancy, and combustion behaviors of EP thermosets were investigated by differential scanning calorimetry (DSC), thermogravimetric analysis (TGA), limited oxygen index (LOI) measurement, vertical burning (UL-94), and cone calorimeter tests. Additionally, the decomposition products in both condensed and gaseous phases were studied to reveal the flame retardant mechanism of DIB.

2. Experimental

2.1. Materials

Diglycidyl ether of bisphenol-A (DGEBA) with an epoxide equivalent weight (EEW) of about 188 g/equiv was purchased from Yueyang Baling Huaxing Petrochemical Co., Ltd (Hunan, China). 1H-Imidazole-4-carbaldehyde, 1,4-benzenediamine, ethanol, and N,N′-dimethyl formamide (DMF) were obtained from Aladdin Industrial Co., Ltd (Shanghai, China). 9,10-Dihydro-9-oxa-10-phosphaphenanthrene-10-oxide (DOPO) was obtained from Huizhou Sunstar Technology Co., Ltd (Guangdong, China). 4,4‘-Diaminediphenyl sulfone (DDS) was provided by Sinopharm Chemical Reagent Co., Ltd (Shanghai, China).

2.2. Synthesis of DIB

In a 100 mL three-necked round-bottomed glass flask equipped with a thermometer, mechanical stirrer, and reflux condenser, 1.92 g of 1H-imidazole-4-carbaldehyde, 1.08 g of 1,4-benzenediamine and 30 mL of DMF were added and stirred at 60 °C for about 4 h. And then, 4.32 g of DOPO and 10 mL of DMF were introduced into the mixture. The mixture was heated to 90 °C and kept at this temperature for 14 h. After the reaction finished, the mixture was distilled to remove DMF. The crude product was respectively washed by ethanol and distilled water for three times, and then vacuum-dried at 60 °C for 24 h. Finally, 4.9 g of ultimate product (82% yield) was obtained. The reaction equation of DIB was shown in Scheme 1.

2.3. Preparation of EP samples

DIB was used as a co-curing agent of DDS to introduce into epoxy resin to prepare a series of reactive flame-retarded EP samples. The detailed formulations of EP samples were presented in Table 1. The preparation process of reactive flame-retarded EP (EP/DDS/DIB) samples was as followed. Firstly, the grinded DIB was introduced into epoxy resin under continuous stirring at 100 °C. Then, the mixture was heated to 120 °C and DDS was added. After stirring for 5 min, the mixture was degassed under vacuum and poured directly into a preheated mold and thermally cured in an air convection oven at 160 °C for 2 h and 180 °C for 5 h. The unmodified EP (EP/DDS) thermoset was prepared by the same procedure without the introduction of DIB. The EP/DOPO sample was prepared by the similar process of the unmodified EP sample but with the addition of DOPO at 80 °C.

2.4. Preparation of EP mixtures for DSC test

1.0 g of EP and 0.9 g of DIB were evenly dispersed in acetone under ultrasonic dispersion. Then, the corresponding EP/DIB mixture was obtained by removing acetone at 50 °C. The preparations of EP/DDS and EP/DDS/DIB mixtures (the mass ratios were

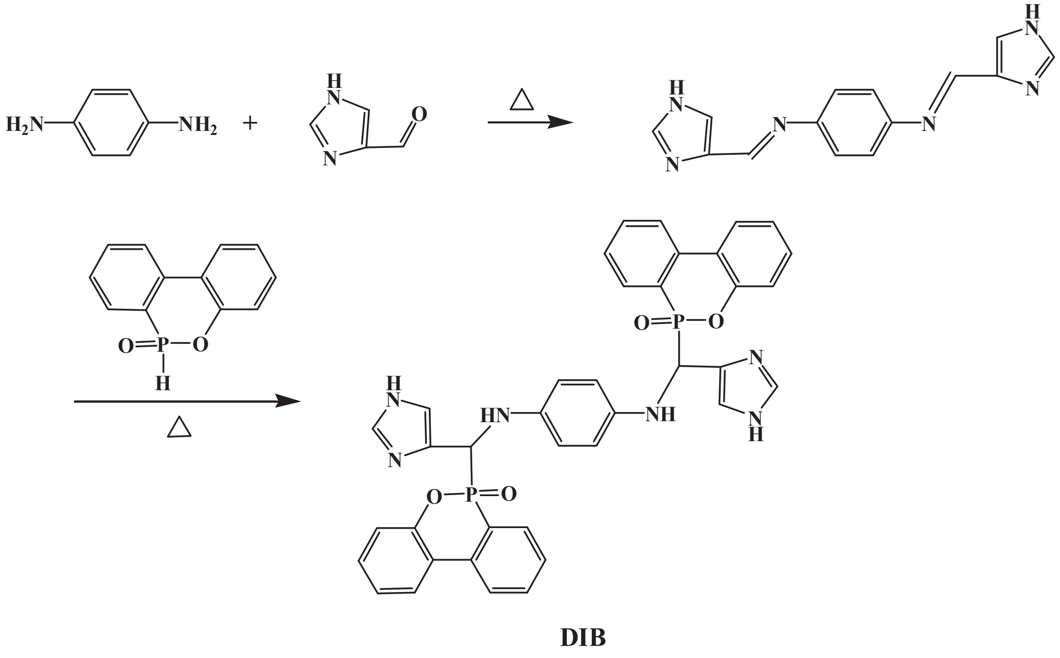

Scheme 1. The synthetic route of DIB.

Table 1
The detailed formulations of EP samples.

Sample code	DGEBA (wt%)	DDS (wt%)	DOPO (wt%)	DIB (wt%)	P content (wt%)
EP/DDS	75.2	24.8	0	0	0
EP/DDS/DOPO	69.9	23.1	7.0	0	1.0
EP/DDS/DIB-0.25	73.9	23.3	0	2.8	0.25
EP/DDS/DIB-0.5	72.6	21.8	0	5.6	0.5
EP/DDS/DIB-0.75	71.2	20.4	0	8.4	0.75
EP/DDS/DIB-1.0	69.8	19.0	0	11.2	1.0

presented in Table 1 were similar to that of EP/DIB mixture.

2.5. Measurements

Fourier Transform Infrared (FTIR) spectra were measured with a Nicolet 6700 infrared spectrometer. The powdered samples were thoroughly mixed with KBr and then pressed into pellets.

^{1}H and ^{31}P NMR spectra were obtained on a Bruker AV400 NMR spectrometer and DMSO-d_6 as the solvent.

Elemental analysis (EA) was performed by a Vario EL cube Elemental Analyzer.

Differential scanning calorimetry (DSC) thermograms were recorded with a Perkin-Elmer DSC 4000 at a heating rate of 10 °C/min from 80 to 240 °C in a nitrogen atmosphere.

The LOI values were measured at room temperature using a JF-3 oxygen index meter (Jiangning Analysis Instrument Company, China) according to ASTM D2863. Dimensions of all samples were $100 \times 6.5 \times 3\ mm^3$. Vertical burning (UL-94) tests were carried out using a NK8017A instrument (Nklsky Instrument Co., Ltd., China) and dimensions of specimens were $130 \times 13 \times 3\ mm^3$ according to the UL-94 test standard. Cone calorimeter measurements were performed using a FTT cone calorimeter according to the ISO 5660 standard under an external heat flux of 50 kW/m^2. The dimensions of samples were $100 \times 100 \times 3\ mm^3$. The measurement for each specimen was repeated three times, and the error values of the typical cone calorimeter data were reproducible within ±5%.

Thermogravimetric analysis (TGA) was performed using a NETZSCH STA449F3 at a heating rate of 10 °C/min from 40 to 800 °C in a nitrogen atmosphere.

Py-GC/MS analysis was carried out with an Agilent 7890/5975 GC/MS. The injector temperature was 250 °C; 1 min at 50 °C then the temperature was increased to 280 °C at a rate of 8 °C/min. The temperature of the GC/MS interface was 280 °C, and the cracker temperature was 500 °C.

Morphological studies on the residual chars were conducted using a JSM-5610LV scanning electron microscope (SEM) at an acceleration voltage of 10 kV. The SEM instrument was integrated with an energy dispersive X-ray (EDX) microanalyser for elemental analysis.

3. Results and discussion

3.1. Synthesis of DIB

The chemical structure of DIB was proved by FTIR, ^{1}H NMR, ^{31}P NMR and EA. The FTIR spectrum of DIB was shown in Fig. 1. As presented in Fig. 1, the absorption band of N–H appeared at 2430-3420 cm^{-1} and the absorption peak of C–H in the imidazole ring appeared at 2869 cm^{-1} [35]. In addition, the absorption peaks at 1660 cm^{-1} and 1511 cm^{-1} were assigned to benzene ring; the absorption peak at 1608 cm^{-1} was assigned to the stretching vibration of C=N in the imidazole ring; the absorption peak at 1448 cm^{-1} was attributed to the stretching vibration of C–N; the absorption peak at 1200 cm^{-1} was attributed to P=O in the phosphaphenanthrene group; the absorption peaks at 927 cm^{-1} and 755 cm^{-1} were attributed to P–O-Ph in the phosphaphenanthrene group. The appearance of these absorption peaks confirmed the existence of imidazole and phosphaphenanthrene groups in the chemical structure of DIB.

The ^{1}H NMR (a) and ^{31}P NMR (b) spectra of DIB were shown in Fig. 2. In the ^{1}H NMR spectrum of DIB, the peak at 11.95 ppm was assigned to the proton of N–H in the imidazole ring; the peaks at 6.75–8.51 ppm were attributed to the proton of benzene ring and the methine in the imidazole ring; the peak at 6.06–6.50 ppm was assigned to the proton of N–H connected with imidazole ring; the peaks at 4.61–5.26 ppm were attributed to proton of the methine connected with phosphaphenanthrene group. It was noteworthy that the integral area ratio of the proton peaks at different chemical shifts was close to the theoretical ratio of different protons in DIB. In order to identify the chemical constitution of DIB, the ^{31}P NMR (b) spectrum of DOPO was introduced into Fig. 2(b). It was evident that the chemical shifts of the phosphorus in DIB were totally different with those in DOPO. In addition, there were two signals appeared at 29.5 and 31.3 ppm in the ^{31}P NMR spectrum of DIB, which was probably attributed to the steric hindrance of phosphaphenanthrene group [26].

The EA result of DIB was listed in Table 2. It was obvious that the test values of C, N and H atoms in DIB were 65.52%, 12.01% and 4.33%, respectively, which were in consistency with the calculated values. On the basis of the analysis above, DIB was successfully synthesized.

3.2. Curing behavior of EP mixtures

The curing behavior of EP mixtures was measured by DSC and

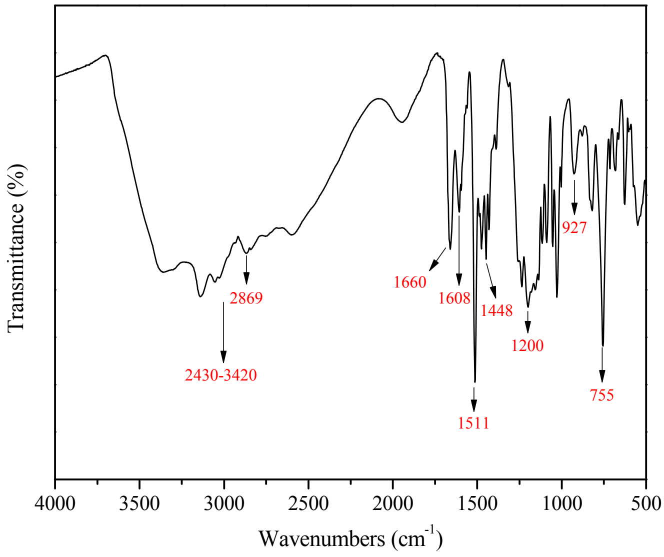

Fig. 1. FTIR spectrum of DIB.

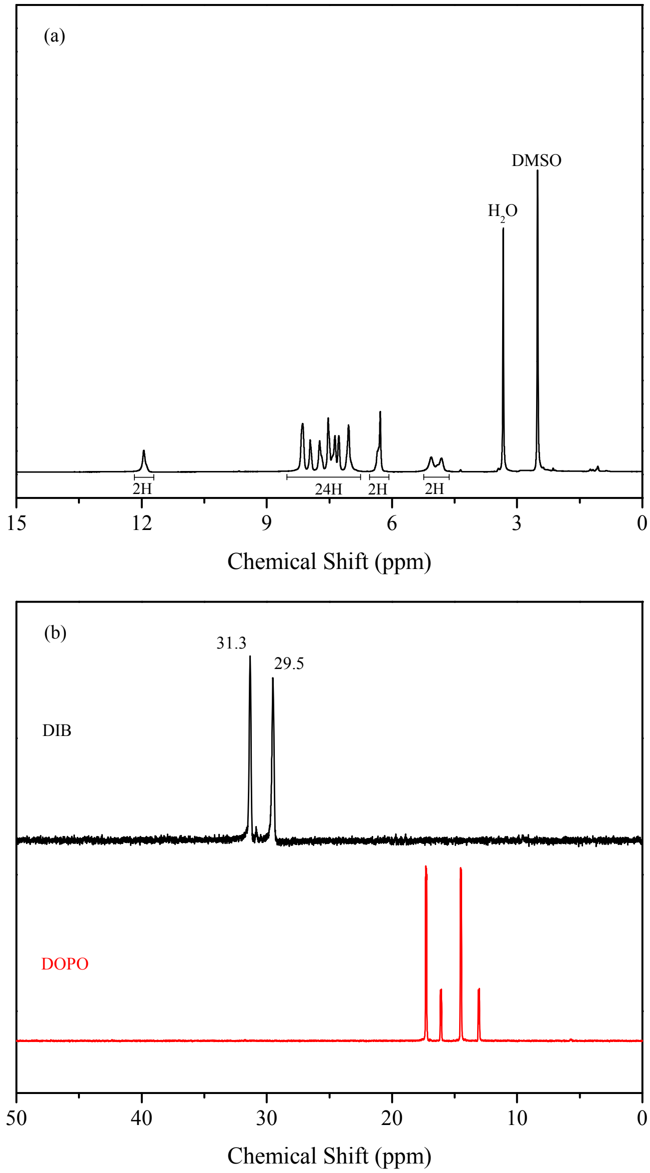

Fig. 2. ^1H NMR of DIB (a) and ^{31}P NMR of DIB and DOPO (b).

the corresponding DSC curves were presented in Fig. 3. As shown in Fig. 3, there was only one exothermic peak corresponding to the curing reaction of DGEBA in each DSC curve. The exothermic peak temperature of EP/DIB mixture was only 177 °C, which was significantly lower than that of EP/DDS mixture (220 °C). In addition, the exothermic peak temperatures of EP/DDS/DIB mixtures were gradually decreased with the increasing content of DIB. The main reason for this phenomenon was that DIB, as an imidazole curing agent, catalyzed the curing reaction of DGEBA [35,36].

3.3. Thermal properties of EP thermosets

It was well known that the glass transition temperature (T_g) was one of the important parameters of representing thermal properties of EP thermoset. The T_g of the prepared EP samples was measured by DSC, and the corresponding DSC curves were presented in Fig. 4. The T_g value of the neat EP thermoset was 208 °C. Due to the steric hindrance of DOPO group, the curing reactivity of N–H in DIB was lower than that in DDS, which led to declines in the T_g values of EP/DDS/DIB samples (182–197 °C). Because of the blocking reaction between DOPO and DGEBA, EP/DDS/DOPO sample possessed the lowest T_g value of all EP samples, which was only 170 °C. Since DIB possessed more than one N–H in its chemical structure, the introduction of it into DGEBA efficiently avoided the blocking reaction. Hence, the T_g values of EP/DDS/DIB samples were significantly higher than that of EP/DDS/DOPO sample. The results suggested that the introduction of DIB was more conducive to maintaining the T_g of EP thermoset than that of DOPO.

Table 2
Elemental analysis result of DIB.

Element sample	C	N	H
Calculated (%)	65.52	12.01	4.33
Found (%)	65.04	11.81	4.42

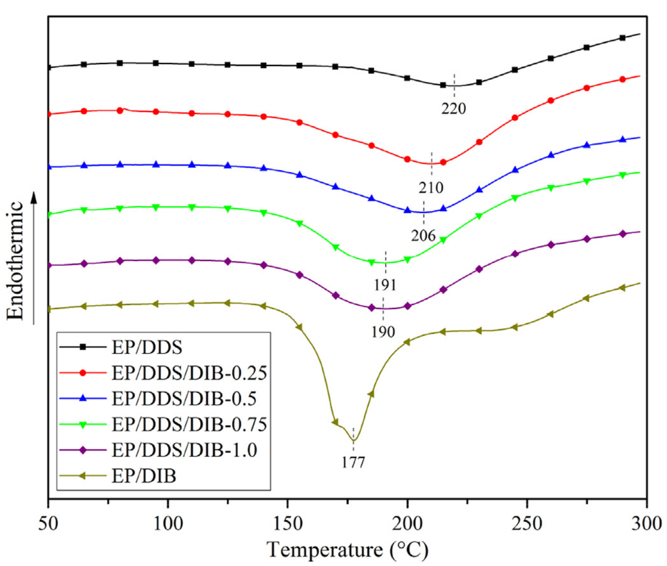

Fig. 3. The DSC curves of EP mixtures.

Thermal stability of DIB and EP samples were studied by TGA under nitrogen atmosphere. The TG and DTG curves of DIB and EP

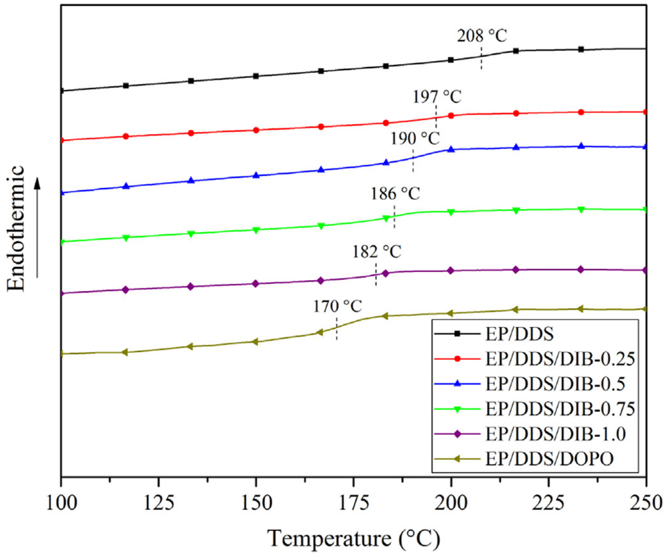

Fig. 4. The T_g of EP thermosets.

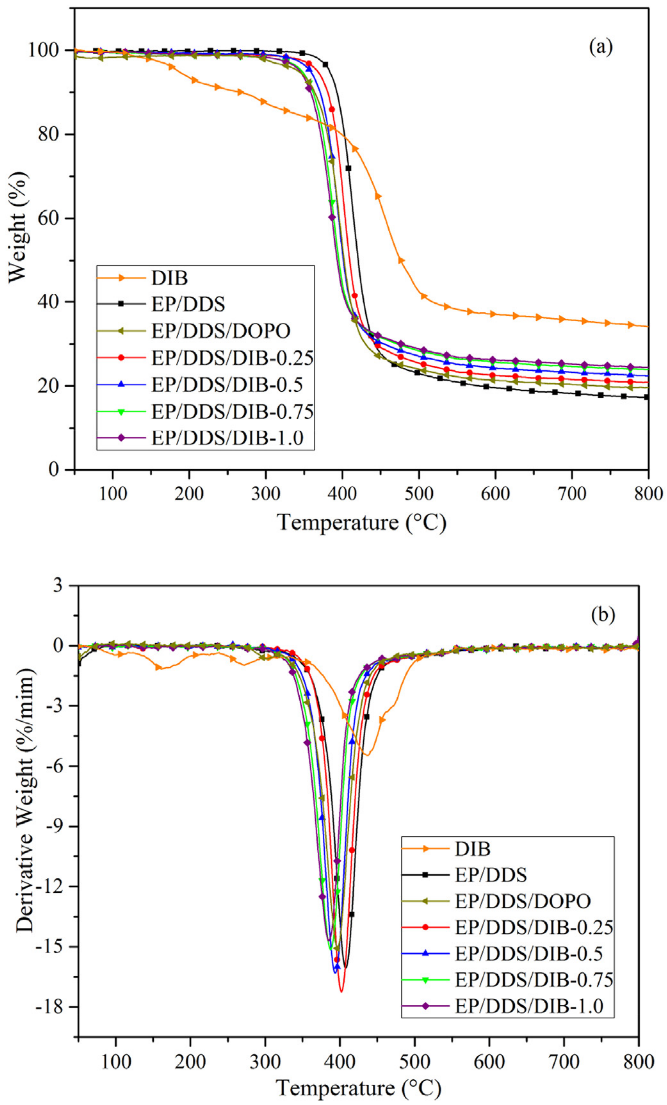

Fig. 5. The TG (a) and DTG (b) curves of EP thermosets.

samples were presented in Fig. 5. The initial mass loss temperature ($T_{5\%}$), the maximum mass loss rate temperature (T_{max}) and the char yield at 800 °C were listed in Table 3.

As shown in Fig. 5 and Table 3, the $T_{5\%}$ and T_{max} of DIB were 190 and 483 °C, respectively. In addition, the char yield of DIB was as high as 34.1% at 800 °C, which indicated that DIB possessed good carbonation property. For EP/DDS/DIB thermosets, the $T_{5\%}$ and T_{max} were gradually decreased with the increasing content of DIB since the phosphate compounds derived from phosphaphenanthrene group of DIB catalyzed the decomposition of EP matrix in the initial stage [1,9]. As the increase of DIB content, the char yields of EP/DDS/DIB thermosets were increased remarkably at 800 °C. To be specific, the char yields of EP/DDS/DIB thermosets were increased by 20.8%–41.6% in comparison to that of EP/DDS thermoset. In addition, the measured values of char yields were much higher than the calculated ones, which indicated that DTA promoted the carbonization of EP matrix. It was obvious that the char yields of EP/DDS/DIB samples were higher than that of EP/DDS/DOPO sample, indicating that there was a synergy between phosphaphenanthrene and imidazole groups on the carbonization of EP matrix. It was deduced that the decomposition products from phosphaphenanthrene group promoted the char formation of EP matrix and imidazole group with good thermal stability retarded the thermal degradation of EP matrix at elevated temperatures.

Table 3
Thermal stability parameters of EP thermosets.

Sample code	$T_{5\%}$ (°C)	T_{max} (°C)	Char yield at 800 °C (%)	
			Measured value	Calculated value
DIB	190	483	34.1	–
EP/DDS	383	408	17.3	–
EP/DDS/DOPO	343	396	19.6	–
EP/DDS/DIB-0.25	368	402	20.9	17.8
EP/DDS/DIB-0.5	358	394	22.5	18.2
EP/DDS/DIB-0.75	347	388	24.0	18.7
EP/DDS/DIB-1.0	344	385	24.5	19.2

3.4. LOI and UL94 rating of EP thermosets

The flame-retardant performance of EP thermosets was investigated by LOI and UL94 tests and the corresponding results were shown in Table 4. The LOI value of EP/DDS thermoset was just 22.5%, and it cannot pass the UL94 test. With the introduction of DIB, the dripping phenomenon was disappeared during the UL94 tests of EP/DDS/DIB thermosets. The addition of DIB brought about the significant increase in LOI value and UL94 rating of EP/DDS/DIB thermosets. For instance, the LOI value of EP/DDS/DIB-1.0 thermoset was as high as 38.5%. Additionally, the UL94 rating of EP/DDS/DIB-0.75 and EP/DDS/DIB-1.0 thermosets both achieved V-0 rating. Only 0.5 wt% phosphorus allowed the LOI value and UL94 rating of EP/DDS/DIB thermoset to be comparable to those of EP/DDS/DOPO thermoset with 1.0 wt% phosphorus. Under the same phosphorus content, the LOI and UL94 rating of EP/DDS/DIB-1.0 thermoset were apparently higher than those of EP/DDS/DOPO thermoset. All these results indicated that DIB was a more efficient flame retardant than DOPO, which endowed EP thermoset with excellent flame-retardant performance under low phosphorus content.

3.5. Combustion behaviors of EP thermosets

The combustion behaviors of EP thermosets were investigated by cone calorimeter test. The characteristic parameters such as the time to ignition (TTI), peak of heat release rate (pk-HRR), average of heat release rate (av-HRR), total heat release (THR), average of effective heat of combustion (av-EHC), average yield of CO (av-COY), average yield of CO_2 (av-CO_2Y), and char yield (CY_{500}) at 500 s were listed in Table 5.

As shown in Table 5, the TTI of EP/DDS thermoset was 47 s. The TTI of EP/DDS/DIB thermosets was lower than that of EP/DDS thermoset, which was probably because of the catalytic effect of DIB on thermal decomposition of EP matrix.

The heat release rate (HRR) curves of all EP thermosets were presented in Fig. 6. In all EP thermosets, EP/DDS thermoset had the

Table 4
The LOI and UL94 results of epoxy thermosets.

Sample code	P content (wt%)	LOI (%)	UL94 (3 mm)	
			Rating	Dripping
EP/DDS	0	22.5	No rating	Yes
EP/DDS/DOPO	1.0	34.1	V-1	No
EP/DDS/DIB-0.25	0.25	32.3	No rating	No
EP/DDS/DIB-0.5	0.5	35.9	V-1	No
EP/DDS/DIB-0.75	0.75	36.8	V-0	No
EP/DDS/DIB-1.0	1.0	38.5	V-0	No

Table 5
The characteristic combustion parameters of epoxy thermosets.

Sample code	TTI (s)	pk-HRR (kW/m^2)	av-HRR (kW/m^2)	THR (MJ/m^2)	av-EHC (MJ/kg)	av-COY (kg/kg)	av-CO_2Y (kg/kg)	CY_{500} (%)
EP/DDS	47	1208	177	80.6	22.2	0.063	1.589	10.4
EP/DDS/DOPO	41	833	155	66.7	19.6	0.095	1.255	20.2
EP/DDS/DIB-0.25	39	918	142	70.5	17.1	0.088	1.334	15.5
EP/DDS/DIB-0.5	37	740	123	60.5	16.5	0.095	1.243	18.1
EP/DDS/DIB-0.75	34	503	119	58.6	15.4	0.108	1.191	19.1
EP/DDS/DIB-1.0	31	517	110	51.6	14.4	0.108	1.132	22.4

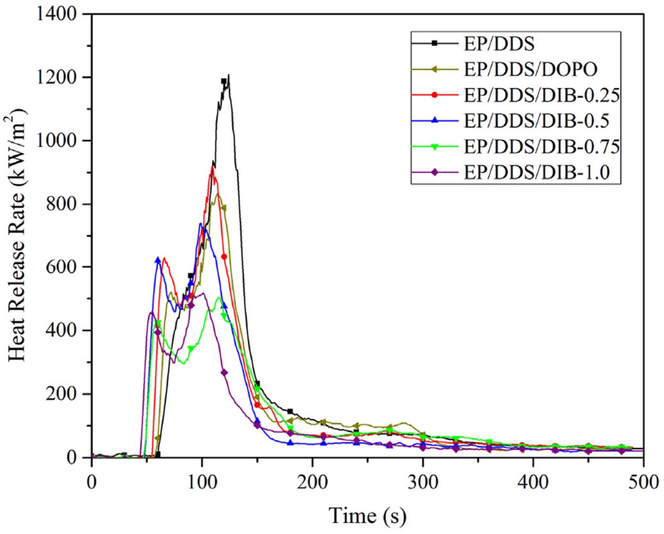

Fig. 6. The HRR curves of EP thermosets.

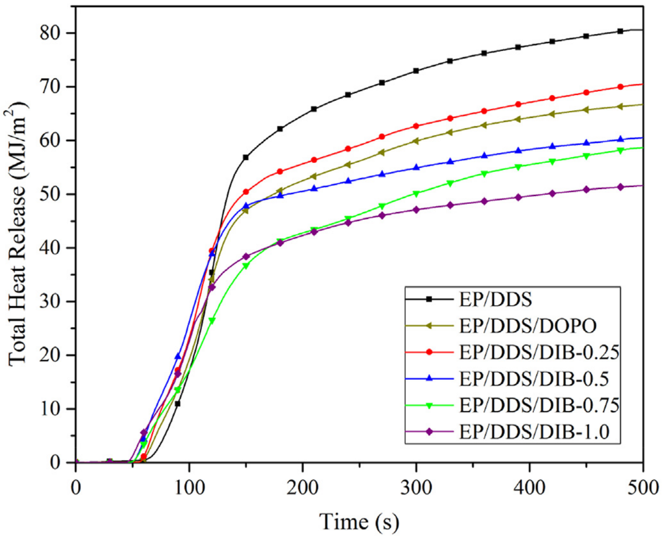

Fig. 7. The THR curves of EP thermosets.

maximum pk-HRR and av-HRR of 1208 and 177 kW/m^2. With the addition of DIB, the pk-HRR and av-HRR of EP/DDS/DIB thermosets were decreased by 24.0%–57.2% and 19.8%–37.9% in comparison to those of EP/DDS thermoset. It was easy to find that the magnitude of pk-HRR and av-HRR reductions was significantly higher than the content of DIB, which demonstrated the outstanding restraining effect of DIB on the combustion intensity of EP matrix. In addition, EP/DDS/DIB-0.5, EP/DDS/DIB-0.75 and EP/DDS/DIB-1.0 thermosets all possessed lower pk-HRR and av-HRR compared with EP/DDS/DOPO thermoset, which further confirmed that DIB had greater flame-retardant efficiency than DOPO. The results further confirmed that DIB was more effective in the suppression of combustion of EP matrix.

The total heat release (THR) curves of EP thermosets were presented in Fig. 7. Similar to the HRR results, the THR of EP/DDS/DIB thermosets at 500 s was significantly decreased with the incorporation of DIB. In detail, the THR of EP/DDS/DIB thermosets was 12.5%–36.0% lower than that of EP/DDS thermoset. Additionally, the EP/DDS/DIB-0.5 and EP/DDS/DIB-0.75 thermosets with lower phosphorus content both had lower THR at 500 s than EP/DDS/DOPO thermoset. All these results further confirmed that DIB endowed EP thermoset with excellent flame-retardant performance.

The av-EHC of EP thermosets was used to evaluate the flame-retardant effect of DIB in gaseous phase, and listed in Table 5. The av-EHC of EP/DDS/DIB thermosets was gradually decreased with the increasing content of DIB. For instance, the av-EHC of EP/DDS/DIB-1.0 thermoset was decreased by 35.1% in comparison to that of EP/DDS thermoset. The remarkable decrease of av-EHC confirmed that DIB exerted flame-retardant effect in gaseous phase. Moreover, the av-COY of EP/DDS/DIB thermosets was gradually increased, while the av-CO_2Y of EP/DDS/DIB thermosets was decreased, which indicated that more and more volatile products burned incompletely. All these results confirmed that DIB exerted the flame-retardant effect and restrained the combustion of EP matrix in gaseous phase.

The char yields (CY_{500}) of all EP thermosets were presented in Table 5 and available to present the condensed-phase flame-retardant effect of DIB. The CY_{500} of unmodified EP/DDS thermoset was only 10.4%. However, with the addition of DIB, the CY_{500} of EP/DDS/DIB thermosets was remarkably increased and 49.0%–115.4% higher than that of EP/DDS thermoset. The results suggested that DIB exerted the flame-retardant effect in condensed phase to promote the carbonization of EP matrix and retard the decomposition.

The cone calorimeter test showed that DIB exerted the gaseous-phase and condensed-phase flame-retardant effects to suppress combustion of EP matrix.

3.6. Py-GC/MS analysis

In order to study the gaseous-phase flame-retardant effect of DIB, the volatile products of DIB and EP/DDS/DIB-1.0 sample were investigated by Py-GC/MS. The typical MS spectra at different retention times were shown in Fig. 8. The pyrolysis process of DIB was drawn from the MS spectra and presented in Scheme 2. As shown in Scheme 2, the initial pyrolytic products of DIB were divided into three principal pieces: p-phenylenediamine pieces ($m/z = 107$ and 108), phosphaphenanthrene-containing pieces ($m/z = 215$ and 216) and imidazole-containing pieces ($m/z = 80$ and 81). Along with the pyrolysis of p-phenylenediamine pieces and the generation of benzene pieces ($m/z = 77$ and 78), inert NH_3 was released. It was well known that PO fragment ($m/z = 47$) derived

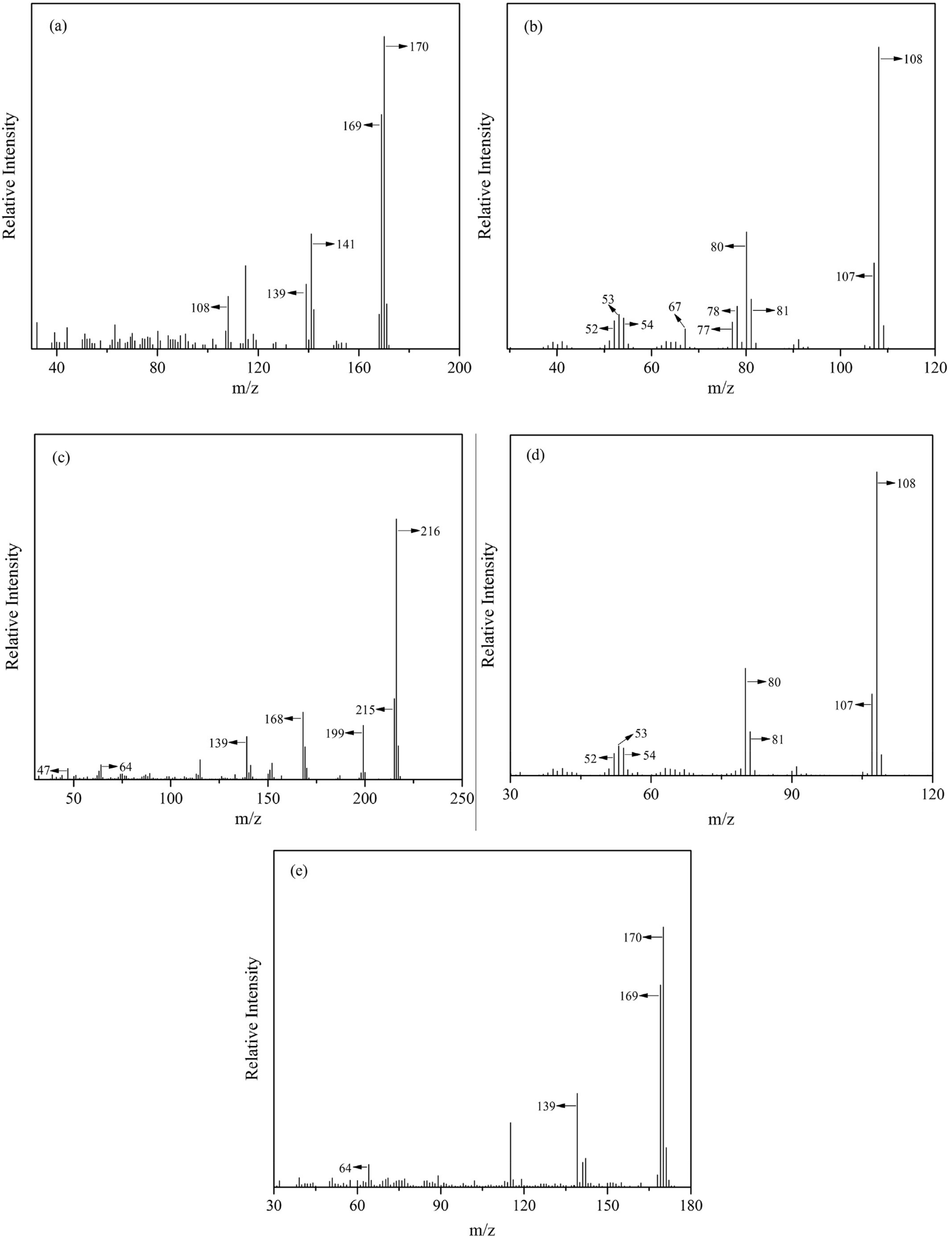

Fig. 8. The typical MS spectra of DIB (a–c) and EP/DDS/DIB-1.0 sample (d, e).

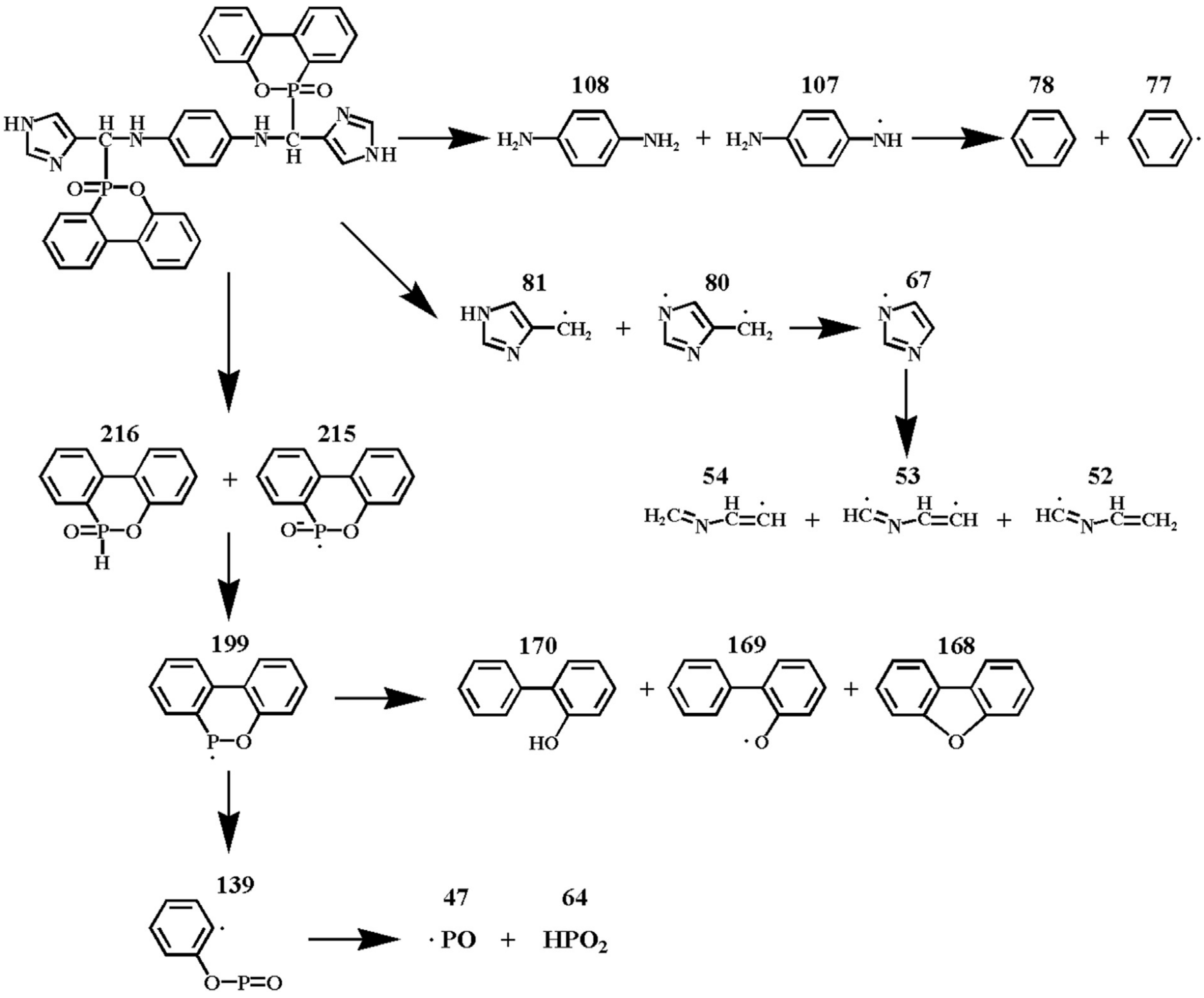

Scheme 2. The pyrolysis process of DIB.

from phosphaphenanthrene-containing pieces was capable of exerting quenching effect in gaseous phase during combustion. In addition, it was speculated that lots of inert gases such as NH_3, nitrogen oxides and so on, were released with the pyrolysis of imidazole-containing pieces. These inert gases were able to exert diluting effect in gaseous phase during combustion. In addition, the fragments ($m/z = 52, 53, 54$ and so on) derived from the pyrolysis of DIB also appeared in the typical MS spectra of EP/DDS/DIB-1.0 sample, which indicated that DIB also decomposed to generate the fragments with quenching or diluting effect in gaseous phase during the pyrolysis of EP/DDS/DIB-1.0 thermoset. The results indicated that as a phosphaphenanthrene- and imidazole-containing flame retardant, DIB exerted the flame-retardant effect in gaseous phase during combustion.

3.7. FTIR of residual chars from UL94 test

The FTIR spectra of char residues of EP/DDS, EP/DDS/DIB-0.75 and EP/DDS/DIB-1.0 thermosets were presented in Fig. 9, which were used to investigate the condensed-phase flame-retardant effect of DIB.

From Fig. 9, the absorption peaks of benzene ring (1592 and 1508 cm^{-1}) were observed in the FTIR spectra of char residues of each EP thermosets. However, there were some new absorption peaks (1619, 1428, 1058, 892, and 754 cm^{-1}) appeared in the FTIR spectra of char residues of EP/DDS/DIB-0.75 and EP/DDS/DIB-1.0 thermosets. It was noteworthy that the peak at 1619 cm^{-1} was attributed to C=N, the peak at 1428 cm^{-1} was attributed to C—N,

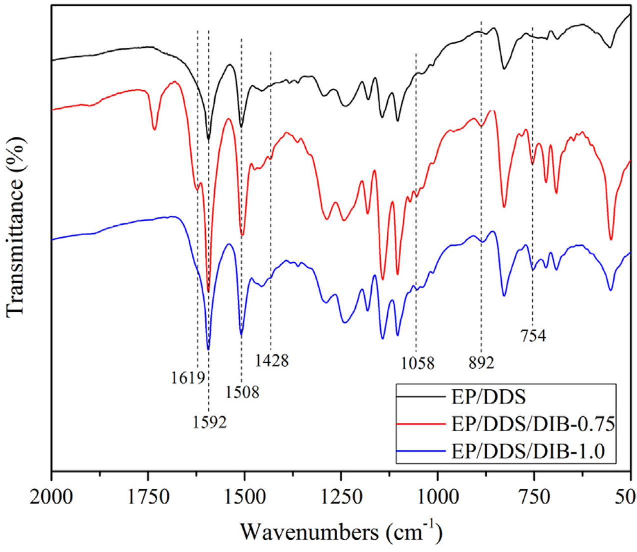

Fig. 9. The FTIR spectra of char residues from UL94 test.

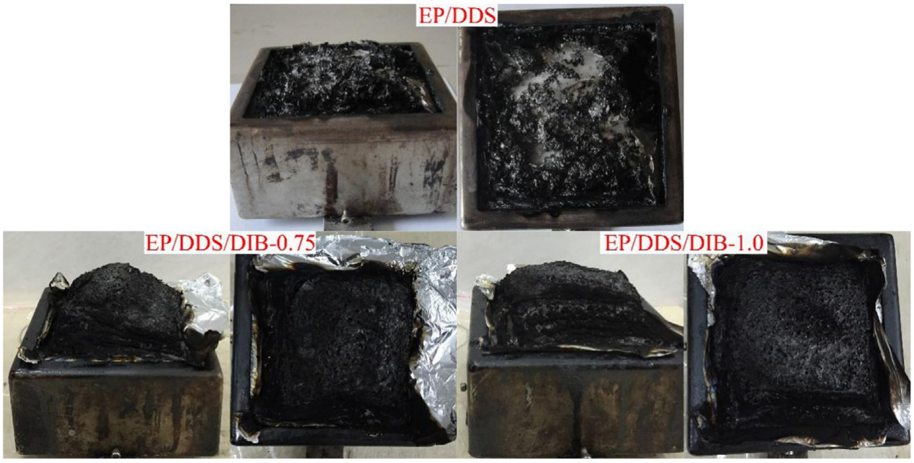

Fig. 10. The digital photographs of char residues from cone calorimeter test.

the peak at 1058 cm^{-1} was attributed to P—O—C, the peak at 892 cm^{-1} was attributed to P—O—P, and the peak at 754 cm^{-1} was attributed to P—O-Ph. The appearance of these new peaks indicated that there were some charring imidazole-containing compounds and phosphate compounds from DIB existed in the char residues. Therefore, the imidazole and phosphaphenanthrene groups of DIB both exerted the condensed-phase flame-retardant effect to promote the carbonization of EP matrix and retard the decomposition during combustion.

3.8. Morphology analysis of residual chars from cone calorimeter test

Macroscopic morphologies of char residues of EP/DDS, EP/DDS/DIB-0.75 and EP/DDS/DIB-1.0 samples were investigated by digital camera and the corresponding digital photographs were shown in Fig. 10. It was easy to find that the char structures of EP/DDS/DIB and EP/DDS samples were totally different. The char structure of EP/DDS sample was broken and loose, but those of EP/DDS/DIB-0.75 and EP/DDS/DIB-1.0 samples were compact and intumescent. Compared with char residue of EP/DDS sample, those of EP/DDS/DIB samples were more conducive to preventing the release of combustible gases and protecting the underlying material. According to this phenomenon, it was inferred that phosphaphenanthrene and imidazole groups synergistically promoted EP matrix to form a protective char layer and exerted the condensed-phase flame retardant effect during combustion.

Microscopic morphologies of char residues of EP/DDS/DIB-0.75 and EP/DDS/DIB-1.0 samples were investigated by SEM, and shown in Fig. 11. The external chars of both EP/DDS/DIB samples were continuous and compact, and the internal chars exhibited honeycomb structure. In addition, some micro-holes existed in the

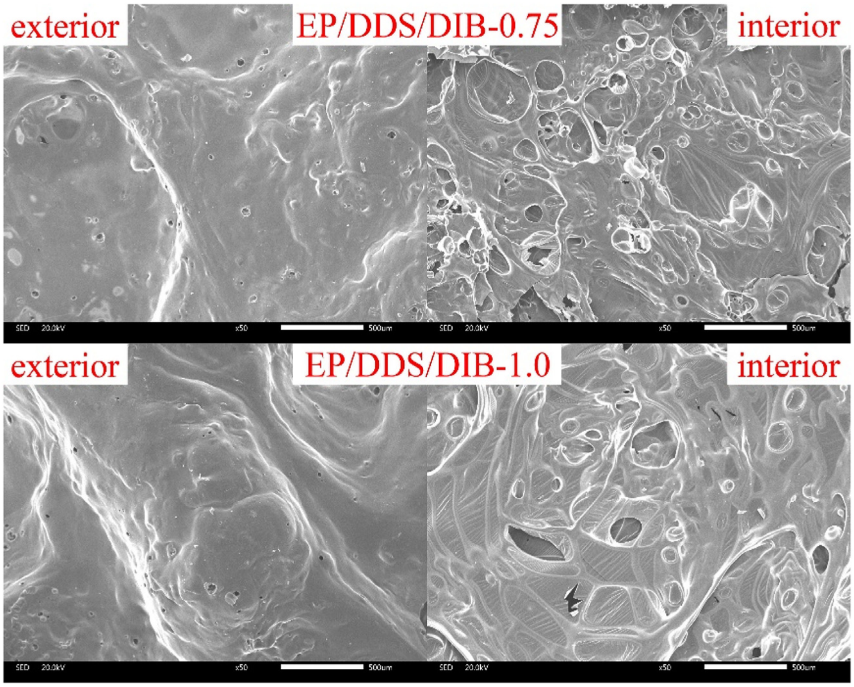

Fig. 11. The SEM images of char residues from cone calorimeter test.

Table 6
EDX results of residual chars.

Sample code	Element content (wt %)				
	C	O	P	N	S
EP/DDS/DIB-0.75	81.67	9.85	0.55	7.36	0.57
EP/DDS/DIB-1.0	79.59	10.29	1.19	8.43	0.50

external chars of both EP/DDS/DIB samples, which was probably due to the concentrated release of radicals and inert gases [9]. During the cone calorimeter test, DIB promoted the formation of compact char layer on the surface of EP samples, and then the pyrolysis gases were wrapped in the underlying char layer to form a honeycomb structure. The structure of this char layer contributed to suppressing the release of pyrolysis gases and transmission of heat during combustion. The results further confirmed the flame-retardant effect of phosphaphenanthrene and imidazole groups in condensed phase.

3.9. *EDX analysis*

The element contents of residual chars of EP/DDS/DIB-0.75 and EP/DDS/DIB-1.0 samples from cone calorimeter test were investigated by EDX and the results were shown in Table 6. With increasing content of DIB, the content of phosphorus, oxygen and nitrogen in the char residue was gradually increased, indicating that more and more phosphate compounds and heat-resistant imidazole groups were retained in the char residue. The EDX results confirmed the effect of phosphaphenanthrene and imidazole groups on the formation of a protective char layer in condensed phase during combustion.

4. Conclusion

In this work, a DOPO-containing imidazole curing agent was successfully synthesized, and served as a co-curing agent of DDS for the preparation of a reactive flame-retardant EP system (EP/DDS/DIB). The introduction of DIB led to the remarkable reduction in curing temperature of epoxy resin due to its catalytic curing action. The T_g and $T_{5\%}$ values of EP sample were gradually decreased, while the char yield was increased with the increasing content of DIB. There was a great enhancement in flame-retardant performance of EP thermoset due to the incorporation of DIB. For instance, the LOI value and UL94 rating of EP/DDS/DIB-1.0 thermoset with only 1.0 wt% phosphorus were as high as 38.5% and V-0, respectively. The pk-HRR, av-HRR and THR of EP/DDS/DIB-1.0 thermoset were decreased by 57.2%, 37.9% and 36.0% in comparison to those of EP/DDS thermoset. During combustion, phosphaphenanthrene and imidazole groups promoted the formation of a protective char layer to suppress the release of pyrolysis gases and transmission of heat in condensed phase, and decomposed to release phosphorus-containing radicals and nitrogen-containing fragments to exert quenching and diluting effects in gaseous phase. Phosphaphenanthrene and imidazole groups of DIB jointly retarded the combustion of EP matrix.

Acknowledgment

This study was funded by the National Defense Pre-Research Foundation of China (Grant No. JCKY2016110C008).

References

[1] Y. Zhou, J. Feng, H. Peng, H. Qu, J. Hao, Catalytic pyrolysis and flame retardancy of epoxy resins with solid acid boron phosphate, Polym. Degrad. Stabil. 110 (2014) 395–404.
[2] Z.-B. Shao, M.-X. Zhang, Y. Li, Y. Han, L. Ren, C. Deng, A novel multi-functional polymeric curing agent: synthesis, characterization, and its epoxy resin with simultaneous excellent flame retardance and transparency, Chem. Eng. J. 345 (2018) 471–482.
[3] S. Qiu, W. Xing, X. Feng, B. Yu, X. Mu, R.K.K. Yuen, Y. Hu, Self-standing cuprous oxide nanoparticles on silica@polyphosphazene nanospheres: 3D nanostructure for enhancing the flame retardancy and toxic effluents elimination of epoxy resins via synergistic catalytic effect, Chem. Eng. J. 309 (2017) 802–814.
[4] T. Ma, C. Guo, Synergistic effect between melamine cyanurate and a novel flame retardant curing agent containing a caged bicyclic phosphate on flame retardancy and thermal behavior of epoxy resins, J. Anal. Appl. Pyrol. 124 (2017) 239–246.
[5] R. Jian, P. Wang, W. Duan, J. Wang, X. Zheng, J. Weng, Synthesis of a novel P/N/S-containing flame retardant and its application in epoxy resin: thermal property, flame retardance, and pyrolysis behavior, Ind. Eng. Chem. Res. 55 (2016) 11520–11527.
[6] B. Perret, B. Schartel, K. Stöß, M. Ciesielski, J. Diederichs, M. Döring, J. Krämer, V. Altstädt, A new halogen-free flame retardant based on 9,10-Dihydro-9-oxa-10-phosphaphenanthrene-10-oxide for epoxy resins and their carbon fiber composites for the automotive and aviation industries, Macromol. Mater. Eng. 296 (2011) 14–30.
[7] R. Sonnier, L. Dumazert, S. Livi, T.K.L. Nguyen, J. Duchet-Rumeau, H. Vahabi, P. Laheurte, Flame retardancy of phosphorus-containing ionic liquid based epoxy networks, Polym. Degrad. Stabil. 134 (2016) 186–193.
[8] W. Zhang, X. Li, R. Yang, Blowing-out effect in epoxy composites flame retarded by DOPO-POSS and its correlation with amide curing agents, Polym. Degrad. Stabil. 97 (2012) 1314–1324.
[9] S. Yang, J. Wang, S. Huo, M. Wang, L. Cheng, Synthesis of a phosphorus/nitrogen-containing additive with multifunctional groups and its flame-retardant effect in epoxy resin, Ind. Eng. Chem. Res. 54 (2015) 7777–7786.
[10] S. Huo, J. Wang, S. Yang, X. Chen, B. Zhang, Q. Wu, B. Zhang, Flame-retardant performance and mechanism of epoxy thermosets modified with a novel reactive flame retardant containing phosphorus, nitrogen, and sulfur, Polym. Adv. Technol. 29 (2018) 497–506.
[11] Y. Qiu, L. Qian, W. Xi, Flame-retardant effect of a novel phosphaphenanthrene/triazine-trione bi-group compound on an epoxy thermoset and its pyrolysis behaviour, RSC Adv. 6 (2016) 56018–56027.
[12] Y.-J. Xu, J. Wang, Y. Tan, M. Qi, L. Chen, Y.-Z. Wang, A novel and feasible approach for one-pack flame-retardant epoxy resin with long pot life and fast curing, Chem. Eng. J. 337 (2018) 30–39.
[13] M. Doğan, A. Yılmaz, E. Bayramlı, Synergistic effect of boron containing substances on flame retardancy and thermal stability of intumescent polypropylene composites, Polym. Degrad. Stabil. 95 (2010) 2584–2588.
[14] L. Yu, L. Chen, L.-P. Dong, L.-J. Li, Y.-Z. Wang, Organic–inorganic hybrid flame retardant: preparation, characterization and application in EVA, RSC Adv. 4 (2014) 17812.
[15] X. He, W. Zhang, R. Yang, The characterization of DOPO/MMT nanocompound and its effect on flame retardancy of epoxy resin, Compos. Appl. Sci. Manuf. 98 (2017) 124–135.
[16] C.H. Lin, Y.C. Chou, W.F. Shiao, M.W. Wang, High temperature, flame-retardant, and transparent epoxy thermosets prepared from an acetovanillone-based hydroxyl poly(ether sulfone) and commercial epoxy resins, Polymer 97 (2016) 300–308.
[17] A. Wirasaputra, X. Yao, Y. Zhu, S. Liu, Y. Yuan, J. Zhao, Y. Fu, Flame-retarded epoxy resins with a curing agent of DOPO-triazine based anhydride, Macromol. Mater. Eng. 301 (2016) 982–991.
[18] S. Huo, J. Wang, S. Yang, B. Zhang, X. Chen, Q. Wu, L. Yang, Synthesis of a novel reactive flame retardant containing phosphaphenanthrene and piperidine groups and its application in epoxy resin, Polym. Degrad. Stabil. 146 (2017) 250–259.
[19] M. El Gouri, A. El Bachiri, S.E. Hegazi, M. Rafik, A. El Harfi, Thermal degradation of a reactive flame retardant based on cyclotriphosphazene and its blend with DGEBA epoxy resin, Polym. Degrad. Stabil. 94 (2009) 2101–2106.
[20] O. Mauerer, New reactive, halogen-free flame retardant system for epoxy resins, Polym. Degrad. Stabil. 88 (2005) 70–73.
[21] Z. Li, R. Yang, Study of the synergistic effect of polyhedral oligomeric octadiphenylsulfonylsilsesquioxane and 9,10-dihydro-9-oxa-10-phosphaphenanthrene-10-oxide on flame-retarded epoxy resins, Polym. Degrad. Stabil. 109 (2014) 233–239.
[22] P. Jiang, X. Gu, S. Zhang, S. Wu, Q. Zhao, Z. Hu, Synthesis, characterization, and utilization of a novel phosphorus/nitrogen-containing flame retardant, Ind. Eng. Chem. Res. 54 (2015) 2974–2982.
[23] M.-J. Xu, G.-R. Xu, Y. Leng, B. Li, Synthesis of a novel flame retardant based on cyclotriphosphazene and DOPO groups and its application in epoxy resins, Polym. Degrad. Stabil. 123 (2016) 105–114.
[24] S. Yang, Y. Hu, Q. Zhang, Synthesis of a phosphorus–nitrogen-containing flame retardant and its application in epoxy resin, High Perform. Polym. 133 (2018), 095400831875649.
[25] L. Qian, Y. Qiu, J. Liu, F. Xin, Y. Chen, The flame retardant group-synergistic-effect of a phosphaphenanthrene and triazine double-group compound in epoxy resin, J. Appl. Polym. Sci. 131 (2014) (n/a-n/a).
[26] P. Wang, Z. Cai, Highly efficient flame-retardant epoxy resin with a novel

DOPO-based triazole compound: thermal stability, flame retardancy and mechanism, Polym. Degrad. Stabil. 137 (2017) 138–150.

[27] P. Wang, L. Xia, R. Jian, Y. Ai, X. Zheng, G. Chen, J. Wang, Flame-retarding epoxy resin with an efficient P/N/S-containing flame retardant: preparation, thermal stability, and flame retardance, Polym. Degrad. Stabil. 149 (2018) 69–77.

[28] R. Jian, P. Wang, L. Xia, X. Yu, X. Zheng, Z. Shao, Low-flammability epoxy resins with improved mechanical properties using a Lewis base based on phosphaphenanthrene and 2-aminothiazole, J. Mater. Sci. 52 (2017) 9907–9921.

[29] S. Yang, J. Wang, S. Huo, M. Wang, J. Wang, Preparation and flame retardancy of a compounded epoxy resin system composed of phosphorus/nitrogen-containing active compounds, Polym. Degrad. Stabil. 121 (2015) 398–406.

[30] S. Huo, J. Wang, S. Yang, J. Wang, B. Zhang, B. Zhang, X. Chen, Y. Tang, Synthesis of a novel phosphorus-nitrogen type flame retardant composed of maleimide, triazine-trione, and phosphaphenanthrene and its flame retardant effect on epoxy resin, Polym. Degrad. Stabil. 131 (2016) 106–113.

[31] Y.-Q. Xiong, X.-Y. Zhang, J. Liu, M.-M. Li, F. Guo, X.-N. Xia, W.-J. Xu, Synthesis of novel phosphorus-containing epoxy hardeners and thermal stability and flame-retardant properties of cured products, J. Appl. Polym. Sci. 125 (2012) 1219–1225.

[32] W. Xu, A. Wirasaputra, S. Liu, Y. Yuan, J. Zhao, Highly effective flame retarded epoxy resin cured by DOPO-based co-curing agent, Polym. Degrad. Stabil. 122 (2015) 44–51.

[33] M. Ghaemy, S.M. Amini Nasab, Synthesis and identification of organosoluble polyamides bearing a triaryl imidazole pendent: thermal, photophysical, chemiluminescent, and electrochemical characterization with a modified carbon nanotube electrode, React. Funct. Polym. 70 (2010) 306–313.

[34] L. Lei, J. Shan, J. Hu, X. Liu, J. Zhao, Z. Tong, Co-curing effect of imidazole grafting graphene oxide synthesized by one-pot method to reinforce epoxy nanocomposites, Compos. Sci. Technol. 128 (2016) 161–168.

[35] D. Lei, W. Ma, L. Wang, D. Zhang, Preparation of 2-ethyl-4-methylimidazole derivatives as latent curing agents and their application in curing epoxy resin, J. Appl. Polym. Sci. 132 (2015).

[36] S. Yang, Q. Zhang, Y. Hu, G. Ding, J. Wang, S. Huo, B. Zhang, J. Cheng, Synthesis of s-triazine based tri-imidazole derivatives and their application as thermal latent curing agents for epoxy resin, Mater. Lett. 216 (2018) 127–130.